Low-Frequency RF Twin-Dipole Applicator for Intermediate Depth Hyperthermia

CAFIERO FRANCONI, CARLO ALBERTO TIBERIO, LUIGI RAGANELLA, AND LUISA BEGNOZZI

Abstract — **In studies on heating deep-seated tumors, various attempts have been made to develop radiofrequency applicators and to confine the controlled volumes into limited sizes at variable useful depths. Results of the present investigation show that the conduction-current mechanism dominates the heating with magnetic dipoles working at frequencies as low as 27 MHz, and that two single-magnetic dipoles forming a loosely coupled pair (twin-dipole applicator) fed by low-frequency, in-phase currents, give a better performance than a single dipole of the same size, due to the phase coherence of the superimposing fields. A number of single-dipole and twin-dipole applicator working at 27 MHz have been developed and given the fundamental tests on phantoms simulating muscle and fat tissues. The results obtained show the feasibility of the proposed applicator to produce a penetration depth up to 7 cm and a power deposition pattern showing a well-defined maximum, which may undergo a controlled shift of a few centimeters in depth. Moreover, the surface overheating may be easily controlled. A circuit design is described that improves the matching and the uniformity of the power deposition pattern. A preliminary calculation in the quasi-static-fields approximation of the electric field induced by the twin-dipole applicator in air is also described.**

I. Introduction

RADIOFREQUENCY (RF) APPLICATORS, on account of the greater penetration depth with respect to microwave applicators, have a great potential in the design of hyperthermia systems for heating deep-seated tissues. Many types of RF applicators have been successfully developed for regional heating, whereas for the treatment of small deep-seated tumors of very frequent clinical occurrence, practical solutions appear to be lacking. The heating mechanism of RF applicators changes according to the frequency used. For low frequencies, the tissue wavelength is longer than the dimensions involved so that the electromagnetic energy in the tissue may be usefully described in terms of quasi-static fields and the heating may be considered mainly due to the Joule effect of conductive currents, since the resistive losses prevail over the dielectric losses [1], [2]. For frequencies that are neither very low nor very high, it is difficult to separate the respective contributions of these two mechanisms and therefore any definition, although useful for practical purposes, is arbitrary.

As far as the mechanism of energy transfer to the dissipative tissue is concerned, another arbitrary distinction is usually made. One mechanism in which the direct interaction of the electric field is important, and the other in which the energy transfer occurs mainly through magnetic field induction [1]. The latter mechanism has been implemented in a number of applicators which offer the advantages of not being invasive, of being easily applied to the body without requiring contact coupling means, so that electromagnetic matching problems to the tissue are minimized. Moreover, these advantages are fully maintained at low radio frequencies. In the low-frequency range, RF radiators have been described as aperture applicators and as dipole sources [1]. Finite-aperture applicators are available at frequencies as low as 50 MHz, either as single open waveguides of various design and aperture dimensions, or as phased arrays [3]–[7]. A variety of configurations of radiating dipoles has been taken into consideration by Morita and Bach Andersen [8]. One of the basic elements considered was RF radiating magnetic-line sources. This theoretical approach has been implemented by J. Bach Andersen in a distributed-current, magnetic-dipole applicator working at 150 MHz, in which the $-j\omega A$ electric-field gives the strongest contribution [9].

All the RF radiating applicators used in hyperthermia work have smaller electric dimensions than the free-space wavelength and generate stronger near fields at lower frequency [10], thus leading to technical problems in the contact coupling and in the electromagnetic matching of the applicators to the body. The resulting penetration depth decreases with the dimensions of the aperture, regardless of the operating frequency, and is further reduced by the point-source effect. The aperture dimensions would, therefore, represent the natural limiting factor at low frequencies [4]. So far, the best penetration depth of a single RF radiator does not seem to exceed 4 cm [1], [2], [4].

If we examine the conductive-current applicators in the low-frequency range and consider only those in which the magnetic-field induction is dominant in the heating mechanism, we find a number of coils of various shapes for local heating derived from the flat "pancake" coil design used in inductive diathermy. Pancake-like coils have been used in various configurations and size with respect to the body [14]–[16]. However, their design does not allow much greater penetration and usually causes superficial overheating of the body tissue [16]. A more uniform heat distribution has been obtained by allowing the coil to scan the tissue surface in order to time average the deposited power

Manuscript received October 7, 1985; revised January 16, 1986. This work was supported in part by a grant from the Consiglio Nazionale delle Ricerche.

C. Franconi, Luigi Raganella, and Luisa Begnozzi are with the Dipartimento di Medicina Interna, II Universitá di Roma, Via O. Raimondo, 00173 Rome, Italy.

C. A. Tiberio is with the Department of Physics, Universitá di Roma, "La Sapienza", 00185 Rome, Italy.

IEEE Log Number 8607851.

over a larger area [17]. For regional heating, the Magnetrode [11], the helical coil [12], and the single-distributed currents sheet of Kato and Ishida [13] have been used. The Magnetrode consists of a single large sheet coil resonating at 13.56 MHz into which the body to be treated should be introduced. The deposited power-distribution curve exhibits a minimum along the coil diameter and is, therefore, intrinsically nonuniform. The helical coil applicator proposed by Kantor and Ruggera [12], gives a homogeneous heating useful for regional hyperthermia. A large rectangular loop made with a 20-cm wide copper ribbon has been used with its plane perpendicular to the body for regional heating at 6 MHz by Kato and Ishida, and the tissue faces the short side of the coil which operates as a single distributed-current sheet [13].

With any low RF magnetic-induction applicator, the deposited power pattern in phantoms of finite size exhibits a minimum in the central volume due to induced current loops and, therefore, heating is not uniform. However, the advantages include deep penetration of energy into the body and minimization of the overheating of the external fat layer, since the induced electric fields lie closely parallel to the external fat–muscle interface [11]–[13], [16].

There is still room for further development of RF applicators to be used for practical local heating of deep-seated tumors of limited size, and those employing low-frequency magnetic induction appear to have a great potential. The aim of the present paper is to report on new magnetic structures and coupling configurations, developed with the aim of controlling the conductive current pattern so that the power will be usefully deposited at variable depths in controlled volumes of definite dimensions. In so doing, the phase of superimposed-induced currents is taken into consideration, in analogy with phased-array techniques.

II. Single-Dipole Applicator

A. Configuration and Circuit Design

We have developed a family of magnetic-induction dipole applicators (Table I) and submitted them to fundamental tests on phantoms of various shape and composition (Table II). As a basic inductor, we have developed a symmetric magnetic dipole consisting of a rectangular loop resonating at 27 MHz. The plane of the loop is perpendicular to the tissue surface, with the longer side of the loop lying parallel to it (Fig. 1(c)). It differs from the radiating magnetic-line source (Fig. 1(a)) developed by Bach Andersen *et al.* [9] in that the conduction currents dominate the heating mechanism. It also differs from the distributed current sheet (Fig. 1 (b)) of Kato and Ishida [13].

The circuit was designed to allow for practical matching and tuning and for uniform heating. The circuit is symmetric with two equal tuning capacitors inserted in the short sides of the loop (Fig. 2(b)). The equivalent circuit is shown together with the current and voltage distributions along the x axis. As the length of the line is only 0.025λ, the current distribution is constant within 1 percent along the line, while the voltage exhibits an almost linear change symmetrical with respect to the center of the line, where it is zero. Thus, the drop in voltage across the capacitors has been halved with respect to an asymmetric circuit of the same size.

Since the magnetic-field contributions from the two short sides are small, the two long parallel conductors are actu-

TABLE I
PHYSICAL DIMENSIONS OF SINGLE AND TWIN-DIPOLE APPLICATIONS

	Single Dipoles				Twin Dipoles			
PROTOTYPE	L	W	TW	H[a]	L	W	H[a]	S
SD-1D	27	2	8[b]	6.5	-	-	-	-
SD-2	27	1	1	6.5	-	-	-	-
TD-A11	-	-	-	-	26	4	6.5	11
TD-A14	-	-	-	-				14
TD-A16	-	-	-	-				16
TD-B14	-	-	-	-	26	2	13.5	14
TD-B16	-	-	-	-				16

* Symbols as for Fig 7, dimensions in cm, resonant frequency 27 MHz, reflecting plane dimensions 40 x 50 cm, the dipole reference systems are shown in Figs 4 and 7, S is the separation between lines, L is the line length, H is the line height from the symmetry plane, W is the individual line width. The z axis is the binary symmetry axis of the dipole, both current lines lie on the x,y plane, if not otherwise stated the x,y planes of both dipole and phantom are parallel, and the two z axes coincide.
[a] The electric equivalent line separation is twice the line height H from the reflecting plane.
[b] Total width of the distributed-current prototype with three equally spaced lines.

TABLE II
DIMENSIONS AND ELECTROMAGNETIC PROPERTIES OF PHANTOMS

	parallelepiped				cylindrical[a]			
PHANTOM	length X	width Y	depth Z	dielectric constant	diameter	dielectric constant	external fat thickness	ref
PM-1	23	36	12	63	-	-	-	[21]
PM-2	50	36	18	70	-	-	-	[22]
CM-1	-	-	-	-	18	70	-	[22]
CMF-2	-	-	-	-	20	70	1.5[b]	[22]

* Dimensions in cm, all simulated muscle phantoms prepared according to the indications given in the cited references with conductivity of .7 $ohm^{-1}m^{-1}$, x,y phantom reference plane on the phantom surface, the axis of a cylindrical phantom is parallel to the x axis, points inside the phantom have a positive z value, the separation of the dipole from the phantom is measured as the position z_D of the dipole x,y plane on the phantom z axis.
[a] Includes the external PVC tube 2 mm thick.
[b] fat conductivity ~ .02 $ohm^{-1}m^{-1}$, fat dielectric constant ~20

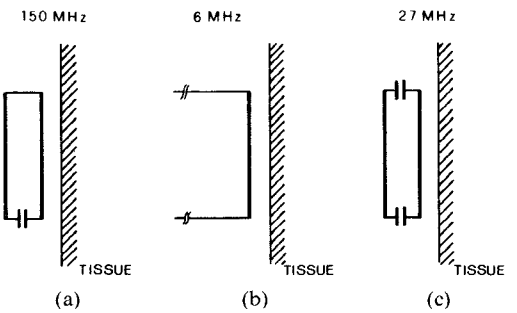

Fig. 1. Schematic view of a single rectangular loop inductor with plane perpendicular to tissue surface, as implemented by various authors: (a) resonant radiating line source for local heating (see Bach Andersen *et al.* [9]); (b) current sheet for regional heating with conductive currents (see Kato and Ishida [13]): (c) resonant symmetric-magnetic dipole for local heating using conductive currents (Tiberio *et al.* [18] and this work).

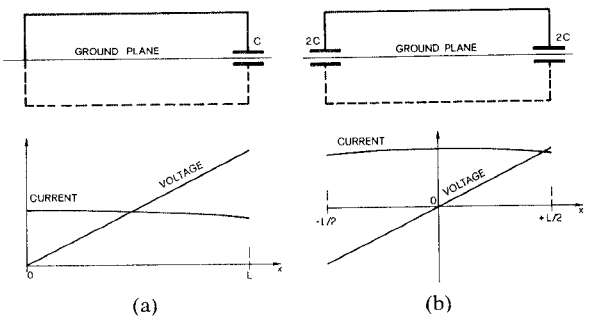

Fig 2 Equivalent electric circuits with voltage and current distributions on lines along x-axis: (a) asymmetric dipole (Bach Andersen *et al.* [9]); (b) symmetric dipole (Tiberio *et al.* [18] and this work).

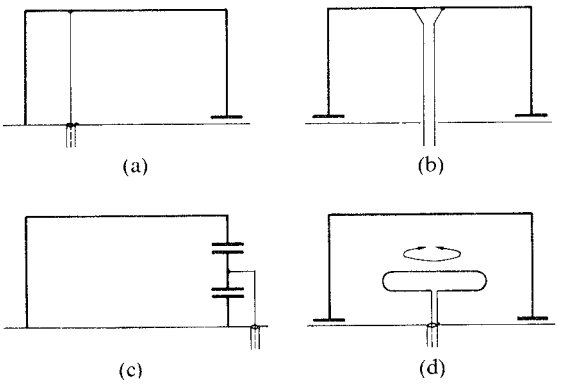

Fig. 3. Some impedance matching circuits useful for magnetic-dipole power feeding: (a) 50-Ω line tapping on asymmetric dipole line; (b) capacitive coupling of asymmetric dipole; (c) center tapping of symmetric dipole line; (d) transformer-like variable coupling of a symmetric dipole.

ally equivalent to a piece of transmission line. The front line carries the current sheet facing the tissue; the back line carrying the return current has been replaced by a reflecting surface [9], which serves also as a ground plane and for physically supporting the tuning capacitors and the coaxial cable connector feeding the inductor. The magnetic-field distribution may be extended along the dipole magnetic axis by a number of close parallel lines carrying in-phase currents, which might be substituted by a single sheet of the same total width carrying a distributed current [9].

Since the load changes dramatically when the dipole gets close to a dissipative tissue, and since further changes are possible during the treatment, fine matching adjustments may be needed during high-power operation. The matching of the line to a power source may be made in many ways. Of the standard RF matching circuits (Fig. 3), the transformer-like circuit (Fig. 3(d)) appeared to be the most satisfactory and was selected. The primary coil is made of a rigid copper loop of suitable area, the plane of which may be easily rotated at the modified panel coaxial connector. The SWR is brought below 1.5 by cut-and-try adjustments of the size and orientation of the feeding loop.

Two versions of the single basic dipole were designed (Table I), both working at 27 MHz. Fig. 4 shows a prototype of model SD-1D. The reflection plane is a printed circuit board 40 cm×50 cm, which operates also as a ground plane. Two parallel-plane capacitors of about 750 pF each are fixed perpendicularly to the conductive side of

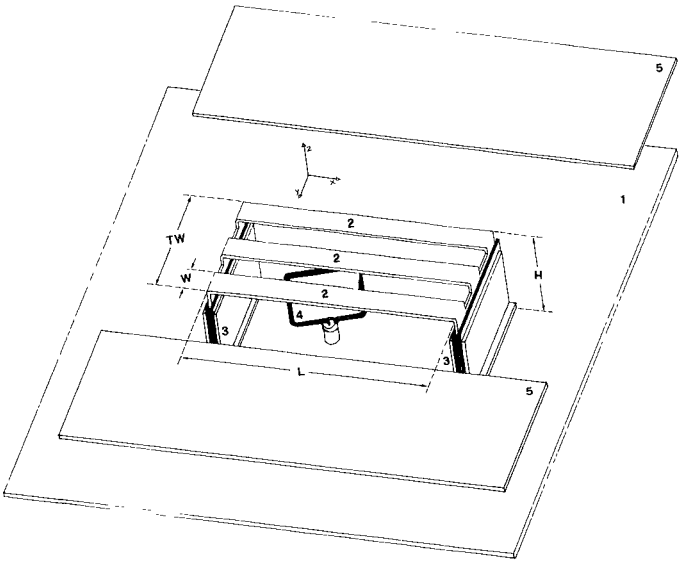

Fig. 4. Schematic view of 27-MHz symmetric single dipole applicator showing 1: reflecting plane, 2: three copper ribbon-like lines, 3: tuning capacitors, 4: variable coupling primary loop, 5: copper sheets for shielding along y-axis direction.

the board, each consisting of two external aluminum plates 6 cm×8 cm facing each other, in which the inner copper electrode is inserted fully, insulated by Teflon sheets from the external electrodes. The two aluminum plates are firmly screwed together and the fine tuning is performed by either shifting the inner electrode or by changing the oscillator frequency. These capacitors are stable and can withstand radio-frequency voltages at powers up to 200 W. Matching and tuning of the applicator were performed by an HP Mod 8410 Network Analyzer. The Q factor of the unloaded dipole is about 180, a value that drops to 30 when the applicator is placed near a dissipative tissue. The average line temperature recorded immediately after power shut-off was about 45°C. Grounded copper sheets bent at an angle of 90° and working as capacitive shields were initially placed above the line ends where the voltage is highest to prevent possible stray fields from overheating the tissue below, but their presence proved to be unimportant and they were removed. However, two flat isolated copper sheets were sometimes used to increase the sharpness of the field decay in the y direction (Figs. 4 and 5(b)). A preliminary report on this dipole has been given elsewhere [18].

The second single dipole was developed to test the effects of the narrow line on the heating pattern. The SD-2 prototype was obtained by substituting the three wide lines of the SD-1D dipole with a single central narrow line, and by a circuit modification for tuning and matching. All the dipoles listed in Table I share the same laboratory technologies developed for intermittent operation.

B. Phantom Tests

The distributed current prototype SD-1D was submitted to fundamental tests with its line at $z_D = 2$ cm from the surface of the muscle phantom PM-1. Dimensions and electromagnetic properties are reported in Table II, together with those of the other phantoms used in this study.

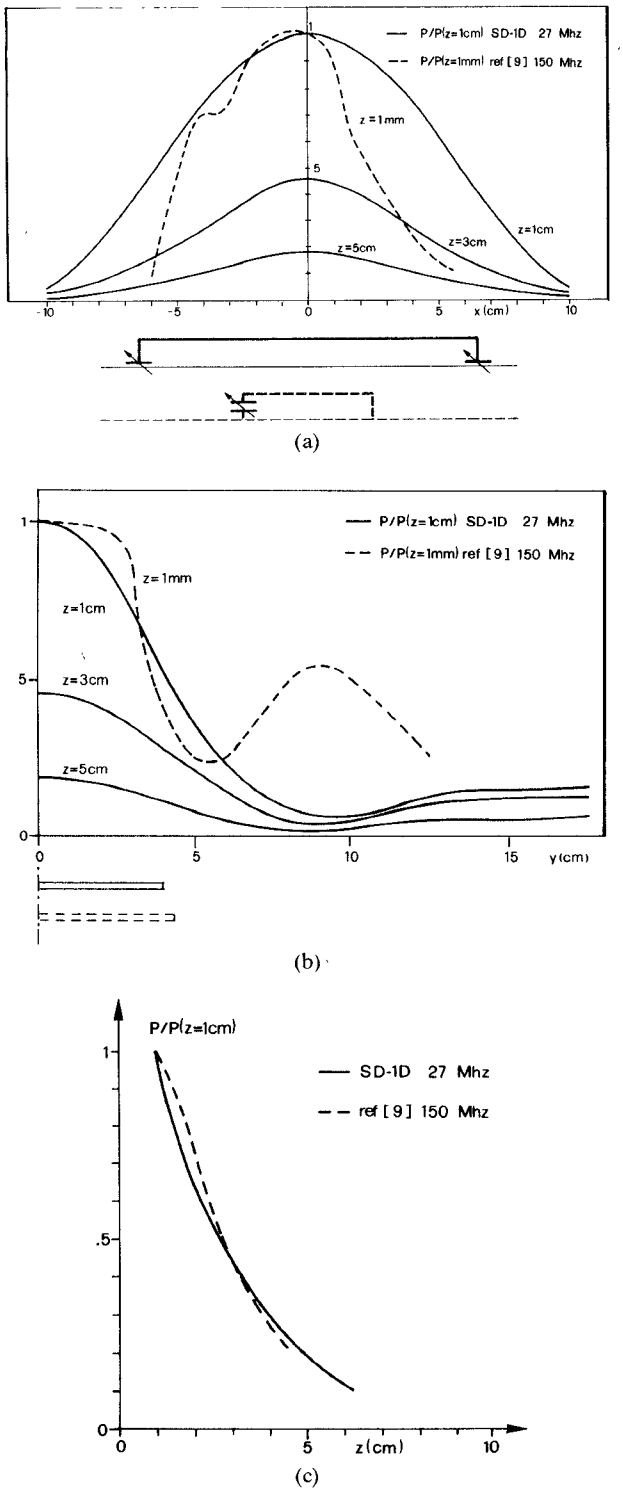

Fig 5. Normalized SAR distributions of single dipole distributed current applicators; dimension of applicators reported on scale: (a) x-z distributions; (b) y-z distributions; (c) central z-axis distributions. (Dashed lines) asymmetric 150-MHz single dipole 9×9 cm on muscle phantom (Bach Andersen *et al.* [9]); curve in (c) has been recalculated and normalized to value at $z = 1$ cm with data from [9]. (Full lines) symmetric 27-MHz single dipole SD-1D on simulated muscle tissue phantom RM-1 with lateral suppression shields (this work).

A wide-band (2–30-MHz) RF power amplifier (G.T. Mod. 200-80-CF), delivering 200 W at 27 MHz and driven by a HP mod. 608 oscillator, was used. The SWR was monitored by two BIRD mod. 43 power meters.

The 27-MHz relative SAR distributions were measured

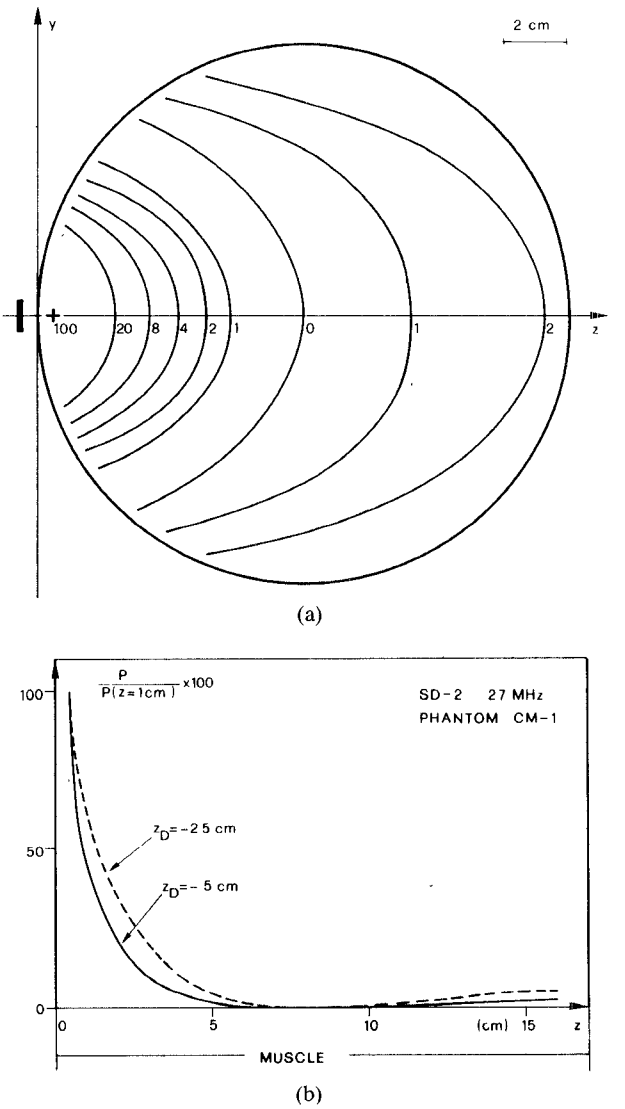

Fig. 6. Normalized SAR distributions of single-dipole applicators on cylindrical phantom CM-1 simulating muscle tissue. (a) Contour map of deposited power for SD-2 dipole at $z_D = -.5$ cm; (b) central z-axis distributions for SD-2 dipole at $z_D = -.5$ cm (full line) and at $z_D = -2.5$ cm (dashed line).

by the temperature-time gradient method (100 W for 10 min) with the temperature distribution mapped over a 2×2-cm grid using a Bailey BAT-12 digital thermometer manually switched over no. 10 Bailey PT6 thermocouples. Temperature rising steps were found to be reproducible within 10 percent. The results obtained at points along the x and y axis at three z depths are plotted in Fig. 5(a) and 5(b), respectively, together with those relative to the 10×9-cm radiative dipole at 150 MHz of Bach Andersen [9]. Even though the x dimension of the two applicators differs, a useful comparison may be made. Firstly, it can be seen that at a lower frequency, the distributions are smoother as expected. Furthermore, symmetrization of the circuit is effective in increasing the x-axis symmetry of the SAR distribution, and also, side shields such as those of Fig. 4 have a beneficial effect. In Fig. 5(c), the penetration depth curve of the SD-1D dipole, reported together with that of the Bach Andersen's dipole [9], shows comparable results.

Since at lower RF frequencies the shape and size of the body play a role in determining the induced current patterns, we tested the narrow-line applicator SD-2 on a cylindrical phantom simulating muscle tissue (phantom CM-1 Table II). The applicator line was facing the phantom at $z_D = .5$ cm. The temperature distribution was mapped over a 1 cm × 1 cm grid on the y, z plane of the cylinder using the method and the temperature monitoring instrumentation described above. The results are shown in Fig. 6(a) in the form of a deposited-power contour map, calculated after proper reduction and processing of the thermometric data. Fig. 6(b) shows the central z-axis distributions for the SD-2 dipole, tested on the CM-1 muscle phantom, and plotted for two values of the line-phantom distance. The null in the deposited power in the phantom central region provides evidence of induced current-loop formation.

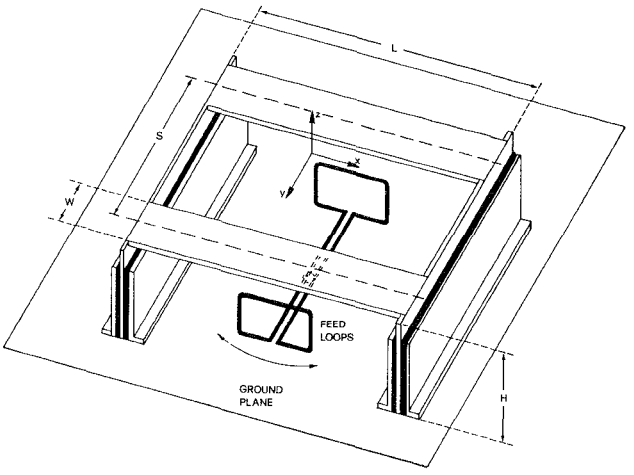

Fig. 7. Schematic view of a twin-dipole applicator developed with two symmetric single-magnetic dipoles. Dimensions of practical applicators are given in Table I.

III. Twin-Dipole Applicator

A. Configuration and Design

Data shown in Figs. 5 and 6 demonstrate that in decreasing the frequency from 150 to 27 MHz, the penetration depth of a single dipole does not change significantly. In order to circumvent the problem, a new type of applicator is proposed in which two parallel narrow-width single-dipole applicators are connected axially at a suitable distance to form a dual-dipole applicator. This system is equivalent to a pair of loosely coupled symmetric rectangular loops carrying equal phase currents of the same intensity. This new applicator (twin-dipole applicator) is illustrated in Fig. 7, where it appears as if we had simply removed the central lines to a distributed current dipole such as the one in Fig. 4, and set the remaining two external lines at the separation desired. With this configuration we obtain a reduction of the overheating of the superficial tissue in the central region, where, in addition, a phase coherent summation of the electric fields induced by the two dipoles takes place, helping to concentrate the deposited power in this region.

In a practical implementation, we had to make sure that both line currents of the twin dipole were in phase, and therefore, the two lines were connected in parallel to the same tuning capacitors and the feeding loop was split into a double-loop system, which may rotate (Fig. 7) for optimal matching. The SWR obtained is below 1.5, and the Q factor of the unloaded applicator is about 150. Five models of twin-dipole applicators were developed in order to assess this new magnetic structure. Physical dimensions are reported in Table I.

B. Phantom Tests

Fundamental tests were carried out with three twin-dipole applicators developed with an increasing value of the separation S between lines (TD-A11, TD-A14, and TD-A16 in Table I) and at different positions z_D from the flat surface of the PM-2 phantom simulating the muscle tissue (see Table II). Measurements were made as reported above for applicator SD-2. The relative power deposition curves along the central z-axis of the phantom are shown in Fig. 8(a) together with the curve of single-dipole SD-1D plotted for comparative purposes. It can be seen that significant increases in penetration depth are obtained over the value of 3.4 cm of the single dipole, reaching 6.5 and 7.3 cm for the two applicators with the larger line distance, the higher value being for the applicator closer to the phantom surface. The relative penetration curves exhibit a convex rather than the usual concave exponential pattern, decreasing only 10 percent at 3.5-cm depth. Moreover, the increased penetration depth is obtained by simply decreasing the twin dipole-phantom distance, a behavior typical of phased-array applicators.

In Fig. 8(b), the power deposition curves measured at $z = 3$-cm depth along the transverse y-axis show a variable degree of overheating below each dipole line, which increases for smaller z_D values. For the TD-A11 twin dipole, overheating is practically absent since the narrower line separation allows more energy to be concentrated in the central part of the tissue. For this applicator, a well-confined volume of about 5 cm × 5 cm of transverse cross section and of about 15-cm length appears to be heated fairly homogeneously, without having performed any optimization. To obtain further penetration, larger separation twin-dipole applicators placed closer to the tissue surface might be used. In this case, however, the upper limit would depend on the maximum heat that can be removed from the tissue surface under the lines.

It is well known that in experimental and clinical situations, the heterogeneity of the tissue and the shape and size of the body may considerably modify the distribution of conductive currents measured on a homogeneous parallel-faced phantom. In order to assess the twin-dipole applicator efficiency under more realistic conditions, we developed two cylindrical phantoms (CM-1 and CMF-2 in Table II) simulating the muscle tissue, one of which is also surrounded by a layer of fat 1.5-cm thick. These were coupled to a pair of new twin-dipole prototypes in which the distance H of the lines from the reflecting plane is 13.5 cm (TD-B14 and TD-B16 in Table I), to allow the cylindrical phantom to further penetrate the applicators (z_D positive).

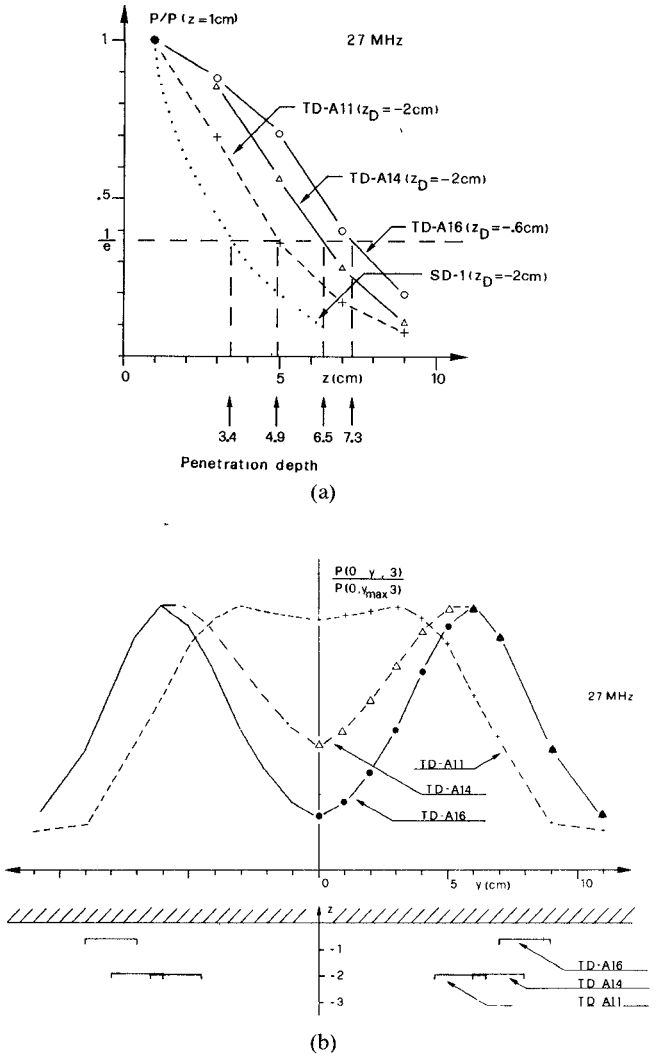

Fig. 8. Relative SAR distributions of twin-dipole applicators at various distances from surface of parallel piped phantom PM-2 simulating muscle tissue. (a) Distribution along central z-axis, normalized to value at $z = 1$-cm depth. Curve at 27 MHZ relative to single dipole SD-1D is plotted for comparison. (b) Distributions along y-axis at $z = 3$ cm depth, normalized to their maximum value.

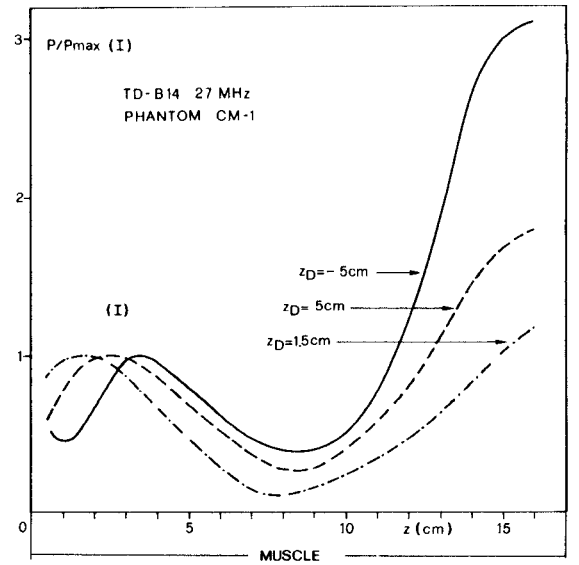

Fig. 9. Relative SAR distributions of twin-dipole TD-B14 facing the cylindrical phantom CM-1 simulating muscle tissue, for three values of line-phantom distance z_D. All values are normalized with respect to first maximum value (1) closest to applicator.

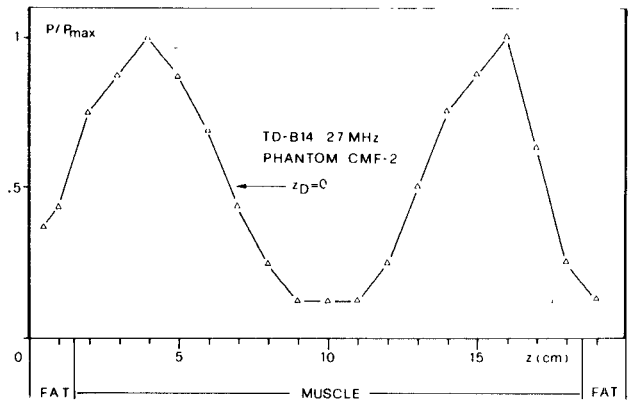

Fig. 10. Relative SAR distributions of twin-dipole TD-B14 facing cylindrical phantom CMF-2 simulating muscle and fat tissues. Curve is normalized to maximum value.

Figs. 9 and 10 show the central z-axis normalized power distributions of applicator TD-14 on muscle phantom CM-1 and on the muscle and fat phantom CMF-2, respectively. A common feature of these curves is their double bell appearance. This type of curve and the extent of the symmetry of the two maxima depend on the boundary conditions for the conductive current loops, such as the definite depth and also the shape and transverse dimensions of the body. In this respect, it can be seen in Fig. 6(b), also referring to a cylindical phantom but for a single dipole, that we have already obtained a null on the z-axis distribution at the phantom center; however in this case, the second maximum is barely noticeable. The two maxima in Fig. 9 are very well defined, and a higher deposition rate is observed for muscle tissue at the surface opposite the applicator, which is not present in Fig. 10 for the phantom with the external fat layer. The results in Fig. 9 further show that the depth of the maxima may be shifted a few centimeters by changing the applicator-phantom separation, a result paralleling that observed for the penetration depth parameter (Fig. 8(a)). The preliminary results of these measurements were reported elsewhere [19].

Temperature measurements integrating the data of Fig. 10 have been taken at the fat-muscle interface. A set of readings was taken along the x direction below the line; the temperature exhibits a maximum at the center of the line, decreasing to 50 percent of the value at both line ends, demonstrating that the electrostatic-field contribution to tissue heating, due to the electric field perpendicular to the fat-muscle interface caused by the voltage drop across the line, is not significant. Such a result could in part be anticipated by an inspection of the results in Fig. 5(a) for a muscle phantom, and by the insignificant effect of electrostatic shielding of line ends reported above.

The set of temperature readings on the central yz plane along the y direction shows a 300-percent increase from the central point at $y = 0$ to the point on the surface below the lines, giving a relative increase of 200 percent with respect to the useful maximum inside the muscle. By means of a mild surface cooling below the lines, such an overheat-

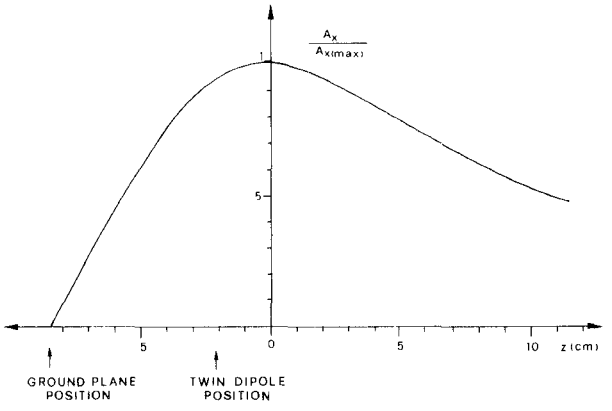

Fig 11 Normalized calculated vector potential A_x in air for a dual-wire rectangular-loop system characterizing twin-dipole configuration. Assumed loop dimensions: $L = 26$ cm; $2H = 13$ cm; loop separation: $S = 14$ cm Maximum of vector potential is calculated to lie at $z = 1.6$ cm outside x, y plane of current carrying wires.

ing is easily brought below the therapeutic temperature on the controlled volume.

C. Quasi-Static Field Calculations

To qualitatively evaluate the efficiency of new configurations of twin-dipole applicators, a preliminary calculation has been made of the induced electric field in air along the central z-axis in the quasi-static-field approximation [23]. Moreover, it was assumed that the effective component of the twin-dipole magnetic field is B_y and, therefore, only the E_x component of the induced electric field is active for heating. Only then does the vector potential component A_x need to be calculated, since along the central z-axis both A_z and A_y do not contribute to B_y and, the behavior of E_x follows that of A_x. The calculation of $A_x(z)$ in air for two rectangular wire loops schematically characterizing the twin dipole has been carried out in the approximation that there are no secondary effects due to the induced currents [20]. The preliminary results for a simplified two-rectangular wire-loop system characterizing a twin-dipole applicator are shown in Fig. 11. It can be seen that A_x exhibits a maximum that appears 1.6 cm beyond the wire position on the z-axis. The vector potential A_x along the central z-axis for these current distributions, such as solenoids and current sheets, should instead exhibit a maximum at the position on the z-axis corresponding to the conducting wire or sheet position [13]. Although the results of these calculations would only partially describe the field behavior inside the conductive material, a comparison of trends is nevertheless possible. In fact, if we were to place a conductive tissue facing all these current distributions, we would have a maximum of the induced electric field increasing inside the first portion of the tissue for the twin dipole, while for single magnetic dipoles and line sources, the electric-field intensity would always decrease monotonically. These preliminary findings are in keeping with the concave behavior (Fig. 8(a)) of the power deposition curves of the twin-dipole applicators.

IV. Summary and Conclusions

A new 27-MHz radiofrequency applicator consisting of a pair of magnetic dipoles (twin-dipole applicator) has been developed, the design of which improves the heating pattern uniformity and allows an easy matching control during operation. This magnetic structure is preferable to single dipoles for heating with radio frequencies limited tissue volumes at intermediate depths. Its working principle takes into consideration the phase coherence of the induced fields, superimposed in a central control volume at depth, not unlike phased-array techniques.

Initial tests carried out in a variety of situations show that with low-frequency twin-dipole applicators, the following results are obtained on a realistic composite muscle and fat cylindrical phantom: i) an effective penetration depth of about 7 cm is reached; ii) the useful power distribution along the z-axis is bell shaped rather than exponential, with a first maximum at a depth of about $z = 4$ cm, which may be used to heat limited tissue volumes; iii) a second maximum appears on the applicator axis at a symmetric position with respect to the phantom center, the extent of which depends upon body shape and electromagnetic parameters; iv) the z position of the maxima may be shifted by a few centimeters by changing the applicator-phantom distance; v) the surface overheating below the lines may be easily controlled. These results, together with those of a preliminary calculation of the quasi-static-induced electric for these magnetic structures, lend further support to the view that the dominant heating mechanism is through induced conduction currents. For a full assessment of the proposed applicator, further systematic studies are therefore necessary for the optimization of the basic magnetic structure in specific applications and on the effects of tissue composition, shape, and size.

Acknowledgment

C. Franconi wishes to thank R. Cavaliere and B. Mondovi for their continuous interest and encouragement, and J. Bach Andersen, G. Gerosa, and F. Bardati for their helpful discussions. The authors wish to express appreciation to O. Adriani, P. Necci, M. Sirolli, and I. Vannucci for their technical assistance.

References

[1] J Bach Andersen, "Electromagnetic heating," in *Proc. 4th Int. Symp Hyperthermic Oncol.*, J. Overgaard, Ed. Taylor & Francis Publ, vol. 2, 1984, pp. 113–128.

[2] M. F. Iskander, "Physical aspects and methods of hyperthermia production by RF currents and microwaves," in *Physical Aspects of Hyperthermia*, G. H. Nussbaum, Ed. American Institute of Physics, New York: 1982, pp 209–230.

[3] P. F. Turner and O. P. Gandhi, "Apparatus for electromagnetic radiation of living tissue and the like," U.S. Patent No. 4 271 848, issued June 9, 1981.

[4] R. H Johnson, J. R. James, J. W. Hand, and R. J. Dickinson, "Compact 27-MHz applicator," *Strahlentherapie*, vol. 9, pp. 537–538, Sept. 1985.

[5] R. Paglione, F. Sterzer, J. Mendecki, E. Friedenthal, and C. Botstein, "27-MHz ridged waveguide applicators for localized hyperthermia treatment of deep-seated malignant tumors," *Microwave J.*, pp. 71–80, Feb. 1981

[6] P. F. Turner, "Regional hyperthermia with an annular-phased

array," *IEEE Trans. Biomed. Eng.*, vol. BME-31, pp. 106–114, Jan. 1984.
[7] A. A. C. Leeuw, J. J. Lagendijk, and J. Schipper, "The design of a clinical deep-body hyperthermia system based on the "coaxial-TEM" applicator," *Strahlentherapie*, vol. 9, p. 529, Sept. 1985.
[8] N. Morita and J. Bach Andersen, "Near-field absorption in a circular cylinder from electric and magnetic line sources," *Bioelectromagnet.*, vol. 3, pp. 253–274, 1982.
[9] J. B. Andersen, A. Baun, K. Harmark, L. Heinzl, P. Raskmark, and J. Overgaard, "New low-profile applicators for local heating of tissues," *IEEE Trans. Biomed. Eng.*, vol. BME-31, pp. 21–27, Jan. 1984.
[10] P. F. Turner and L. Kumar, in *Nat. Cancer Inst. Monogr.*, vol. 61, pp. 521–523, 1982.
[11] F. K. Storm, R. S. Elliott, W. H. Harrison, and D. L. Morton, "Clinical RF hyperthermia by magnetic-loop induction: A new approach to human cancer therapy," *IEEE Trans. Microwave Theory Tech.*, vol. MTT-30, pp. 1149–1158, Aug. 1982.
[12] P. S. Ruggera and G. Kantor, "Development of a family of RF helical coil applicators which produce transversely uniform axially distributed heating in cylindrical fat-muscle phantoms," *IEEE Trans. Biomed. Eng.*, vol. BME-31, pp. 98–106, Jan. 1984.
[13] H. Kato and T. Ishida, "A new inductive applicator for hyperthermia," *J. Microwave Power*, vol. 18, no. 4, pp. 331–336, 1983.
[14] R. D. Zwicker and E. S. Sternick, "Thermal energy deposition from a single-loop RF whole-body applicator," *Med. Phys.*, vol. 10, no. 1, pp. 104–108, Jan./Feb. 1983.
[15] J. W. Hand, J. W. Ledda, and N. T. S. Evans, "Considerations of radiofrequency heating for localized hyperthermia," *Phys. Med. Biol.*, vol. 27, pp. 1–16, 1982.
[16] A. W. Guy, J. F. Lehmann, and J. B. Stonebridge, "Therapeutic applications of electromagnetic power," *Proc. IEEE*, vol. 62, pp. 55–75, Jan. 1974.
[17] M. Von Ardenne, "Krebs-mehrschritt-therapie," *Deutsches Arzteblatt*, vol. 33, no. 13, pp. 1560–1566, Aug. 1981.
[18] C. A. Tiberio, L. Raganella, and C. Franconi, "Symmetric pure induction 27-MHz applicator," in *Proc. 2nd Int. Conf. Applications Phys. Med. Bio.*, C. Franconi *et al.*, Eds., 1984, p. 585, World Science Publ.
[19] C. Franconi, L. Raganella, and C. A. Tiberio, "Linear induction applicator," presented at 1984 IV Int. Symp. Hyperthermic Oncol., Aahrus, DK, July 2–6, 1984.
[20] E. Weber, *Electromagnetic Fields*, New York: J. Wiley & Sons, 1950, p. 133.
[21] A. W. Guy, "Analyses of electromagnetic fields induced in biological tissue by thermographic studies on equivalent phantom models," *IEEE Trans. Microwave Theory Tech.*, vol. MTT-19, pp. 205–214, Feb. 1971.
[22] M. G. Bini, A. Ignesti, L. Millanta, R. Olmi, N. Rubino, and R. Vanni, "The polyacrylamide as a phantom material for electromagnetic hyperthermia studies," *IEEE Trans. Biomed Eng.*, vol. BME-31, pp. 317–322, Mar. 1984.
[23] J. C. Lin, A. W. Guy, and C. C. Johnson, "Power deposition in a spherical model of man exposed to 1–20 MHz electromagnetic fields," *IEEE Trans. Microwave Theory Tech.*, vol. MTT-21, pp. 791–797, Dec. 1973.

Cafiero Franconi was born in Arcevia, Italy, in 1929. He received the degree in physics in 1956. His thesis concerned the R&D of a pulsed ultrasonic apparatus for measuring the absorption coefficient in liquids. In 1958 and 1959, he was a Research Fellow and an A. A. Noyes Fellow in the Chemistry Department of Stanford University and Cal-Tech, respectively.

From 1960 to 1965, he was a Lecturer in radiofrequency spectroscopy at the University of Rome, Italy, and a Professor of Molecular Spectroscopy at the University of Cagliari. From 1970 to 1975, he was a Professor of Physical Chemistry at the University of Venice, where he worked in the areas of molecular biophysics, ultrasound and NMR relaxation in liquids, and the R&D of NMR, ESR and double resonance instrumentation, and of methods of assay in biologically active species. In 1975, he joined the Faculty of Medicine of Rome University "La Sapienza" as Professor of Medical Physics, and in 1982, he moved to the II University of Rome, where he is currently Professor of Medical Physics and Chairman of the Department of Internal Medicine. Current research interests include hyperthermia, short-term simulation of the cardiovascular system, and the R&D of an *S*-Band ESR spectrometer for biological samples. He holds international patents on microwave spin inductors and on a method of assay of biological molecules. He is European Editor of *Clinical Physics and Physiological Measurements*, and co-Director of the Advanced Study Institute on "Physics and Technology of Hyperthermia" to be held in Urbino, Italy, 1986.

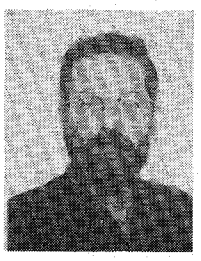

Carlo Alberto Tiberio was born in Rome, Italy, in 1921. He received the M.D. degree in physics from the University of Rome in 1947.

Since then, he has worked at the Physics Department of Rome University on various research projects including ionospheric radiopropagation and solar energy conversion, and at the Physical Chemistry Department on nuclear and electron spin resonance. He is currently engaged in a research project in electromagnetic hyperthermia.

From 1962 to 1970, he was consultant to Varian A. G. in Switzerland for the NMR/ESR instrumentation. In 1958, he was appointed Senior Lecturer of Applied Physics and successively Associated Professor at the University "La Sapienza" of Rome.

Luigi Raganella was born in Rome, Italy, on January 2, 1953. He received the degree in physics from the University of Rome in 1983.

He has been with the Medical Physics Section of the Department of Internal Medicine of the II University of Rome as National Council of Research Fellow since that time, attending also the post-graduate school in medical physics. His research interests are hyperthermia and electromagnetic waves and their interaction with biological systems.

Luisa Begnozzi was born in Milan, Italy, in 1953. She received the degree in physics in 1977 from the University of Milan. She has been attending the post-graduate school in medical physics at the II University of Rome since 1983, while working on radiofrequency hyperthermia.